Nonlinear Dyn
DOI 10.1007/s11071-007-9302-6

ORIGINAL PAPER

2:1 and 1:1 frequency-locking in fast excited van der Pol–Mathieu–Duffing oscillator

Mohamed Belhaq · Abdelhak Fahsi

Received: 21 June 2007 / Accepted: 10 September 2007
© Springer Science+Business Media B.V. 2007

Abstract The frequency-locking area of 2:1 and 1:1 resonances in a fast harmonically excited van der Pol–Mathieu–Duffing oscillator is studied. An averaging technique over the fast excitation is used to derive an equation governing the slow dynamic of the oscillator. A perturbation technique is then performed on the slow dynamic near the 2:1 and 1:1 resonances, respectively, to obtain reduced autonomous slow flow equations governing the modulation of amplitude and phase of the corresponding slow dynamics. These equations are used to determine the steady state responses, bifurcations and frequency-response curves. Analysis of quasi-periodic vibrations is carried out by performing multiple scales expansion for each of the dependent variables of the slow flows. Results show that in the vicinity of both considered resonances, fast harmonic excitation can change the nonlinear characteristic spring behavior from softening to hardening and causes the entrainment regions to shift. It was also shown that entrained vibrations with moderate amplitude can be obtained in a small region near the 1:1 resonance. Numerical simulations are performed to confirm the analytical results.

Keywords Fast excitation · Self-excitation · Parametric forcing · Frequency-locking

M. Belhaq (✉)
Laboratory of Mechanics, University Hassan II-Aïn Chock, PB 5366, Maârif, Casablanca, Morocco
e-mail: mbelhaq@hotmail.com

A. Fahsi
Department of Mathematics, FST Mohammadia, University Hassan II-Mohammadia, Mohammadia, Morocco

1 Introduction

In this paper, we study the effect of a fast harmonic excitation (FHE) on the entrainment area of the 2:1 and 1:1 resonances in a van der Pol–Mathieu–Duffing oscillator. Entrainment or frequency-locking phenomenon was investigated by many authors. Tondl [1] investigated self- and parametrically (SP) excited oscillators with one and two degrees of freedom and provided entrainment areas. Schmidt [2] analyzed interaction of SP excited vibrations while Szabelski and co-workers [3, 4] examined the interaction between parametric, nonparametric and self-excited vibrations in systems with one or two degrees of freedom. Belhaq and co-workers [5–7] studied SP excited oscillator near the strong resonances 1:1, 2:1, 3:1 and 4:1 and determined the entrained oscillations and the quasi-periodic zones. Yano [8, 9] considered vibrations of SP excited systems and determined amplitude modulation of the quasi-periodical vibrations and synchronized motion while Abouhazim et al. [10] investigated entrainment near the 2:2:1 resonance in an SP quasi-periodic Mathieu oscillator. Recently, Pandey et al.

[11] studied frequency-locking in a forced Mathieu–van der Pol–Duffing system near the principal resonances and provided application in optically driven MEMS resonators [12].

The present paper analyzes the effect of a FHE on the dynamic of a van der Pol–Mathieu–Duffing oscillator. Attention will be focused on the influence of FHE on the frequency-locking area corresponding to the 1:1 and 2:1 resonances. The study of the FHE effects on the slow dynamic of mechanical systems has been considered in recent years [13, 14]. A such excitation can affect certain characteristics of systems such as equilibrium stability [15], linear stiffness [16], natural frequencies [17], damping [18], stick-slip dynamics [19, 20], symmetry breaking [21] and Hopf bifurcation [22, 23]. For details on FHE effect, see [24].

The paper is organized as follows: In Sect. 2, we use an averaging technique to derive an SP excited equation governing the slow dynamic of the oscillator. Section 3 is devoted to the 2:1 resonance case. The multiple scales method is applied on the slow dynamic to derive an autonomous slow flow. Analysis of equilibrium points of this slow flow provides analytical approximations of the amplitude of the entrained response. The limit cycle is investigated by constructing analytical expressions of the periodic solution of the slow flow. We perform numerical study and we compare the obtained results to the analytical finding for validation. In Sect. 4, similar analysis is performed for the 1:1 resonance case. Section 5 concludes the work.

2 Slow motion

Consider the following van der Pol–Mathieu–Duffing oscillator subjected to a FHE

$$\ddot{x} + (1 - h\cos\omega t)x - \left(\alpha - \beta x^2\right)\dot{x} - \gamma x^3 = a\Omega^2 \cos x \cos\Omega t, \tag{1}$$

where damping α, β, nonlinearity γ and excitation amplitudes h and a are small. An overdot denotes differentiation with respect to time t. We assume that the frequency Ω is large compared to ω such that resonance phenomena with the frequency Ω are avoided.

To analyze the influence of high-frequency excitation on the slow dynamic of system (1), we use the method of direct partition of motion (DPM) [25] by introducing two different time scales: a fast time $T_0 = \Omega t$ and a slow time $T_1 = t$. We split up $x(t)$ into a slow part $z(T_1)$ and a fast part $\epsilon\phi(T_0, T_1)$ as follows

$$x(t) = z(T_1) + \epsilon\phi(T_0, T_1), \tag{2}$$

where z describes slow main motions at time-scale of oscillations, $\epsilon\phi$ stands for an overlay of the fast motions and ϵ indicates that $\epsilon\phi$ is small compared to z. Since Ω is considered as a large parameter we choose $\epsilon \equiv \Omega^{-1}$, for convenience. The fast part $\epsilon\phi$ and its derivatives are assumed to be 2π-periodic functions of fast time T_0 with zero mean value with respect to this time, so that $\langle x(t)\rangle = z(T_1)$ where $\langle\rangle \equiv \frac{1}{2\pi}\int_0^{2\pi}()\,dT_0$ defines time-averaging operator over one period of the fast excitation with the slow time T_1 fixed.

Introducing $D_i^j \equiv \frac{\partial^j}{\partial^j T_i}$ yields $\frac{d}{dt} = \Omega D_0 + D_1$, $\frac{d^2}{dt^2} = \Omega^2 D_0^2 + 2\Omega D_0 D_1 + D_1^2$ and substituting (2) into (1) gives

$$\begin{aligned}
&\epsilon^{-1} D_0^2\phi + 2D_0D_1\phi + \epsilon D_1^2\phi + D_1^2 z \\
&\quad + (1 - h\cos\omega T_1)(z + \epsilon\phi) \\
&\quad - \left(\alpha - \beta(z + \epsilon\phi)^2\right)(D_0\phi + \epsilon D_1\phi + D_1 z) \\
&\quad - \gamma(z + \epsilon\phi)^3 \\
&\qquad = \epsilon^{-1}(a\Omega)\cos(z + \epsilon\phi)\cos T_0.
\end{aligned} \tag{3}$$

Averaging (3) leads to

$$\begin{aligned}
&D_1^2 z + (1 - h\cos\omega T_1)z - \left(\alpha - \beta z^2\right)D_1 z - \gamma z^3 \\
&\quad = \epsilon^{-1}(a\Omega)\langle\cos(z + \epsilon\phi)\cos T_0\rangle.
\end{aligned} \tag{4}$$

Subtracting (4) from (3) yields

$$\begin{aligned}
&\epsilon^{-1} D_0^2\phi + 2D_0D_1\phi + \epsilon D_1^2\phi + (1 - h\cos\omega T_1)\epsilon\phi \\
&\quad - \left(\alpha - \beta z^2\right)(D_0\phi + \epsilon D_1\phi) \\
&\quad + \beta\left(2\epsilon\phi + \epsilon^2\phi^2\right)(D_0\phi + \epsilon D_1\phi) \\
&\quad - \gamma\left(3\epsilon z^2\phi + 3\epsilon^2 z\phi^2 + \epsilon^3\phi^3\right) \\
&\qquad = \epsilon^{-1}(a\Omega)\cos(z + \epsilon\phi)\cos T_0 \\
&\qquad\quad - \epsilon^{-1}(a\Omega)\big\langle\cos(z + \epsilon\phi)\cos T_0\big\rangle.
\end{aligned} \tag{5}$$

An approximate expression for $\epsilon\phi$ is obtained from (5) by considering only the dominant terms of order ϵ^{-1} as

$$D_0^2\phi = (a\Omega)\cos z\cos T_0, \tag{6}$$

where it is assumed that $a\Omega = O(\epsilon^0)$. The stationary solution to the first order for ϕ is written as

$$\epsilon\phi = -a\cos z\cos T_0. \tag{7}$$

The equation governing the slow motion is derived from (4). Inserting $\cos(z+\epsilon\phi) = \cos z - \epsilon\phi\sin z + O(\epsilon^2)$ into (4) and retaining the dominant terms of order ϵ^0, we obtain

$$\begin{aligned} &D_1^2 z + (1 - h\cos\omega T_1)z - \big(\alpha - \beta z^2\big)D_1 z - \gamma z^3 \\ &\quad = -(a\Omega)\sin z\langle\phi\cos T_0\rangle. \end{aligned} \tag{8}$$

Inserting ϕ from (7) and using that $\langle\cos^2 T_0\rangle = 1/2$, we find the approximate equation for slow motions

$$\begin{aligned} &D_1^2 z + (1 - h\cos\omega T_1)z - \big(\alpha - \beta z^2\big)D_1 z - \gamma z^3 \\ &\quad = \frac{1}{2}(a\Omega)^2\cos z\sin z, \end{aligned} \tag{9}$$

which is similar to the original equation (1) in which the nonautonomous term $a\Omega^2\cos x\cos\Omega t$ is replaced by the autonomous one $\frac{1}{2}(a\Omega)^2\cos z\sin z$. We focus the analysis on small vibrations around the origin by expanding in Taylor's series the terms $\sin z \simeq z - z^3/6$ and $\cos z \simeq 1 - z^2/2$. Keeping only terms up to order three in z, (9) becomes

$$\begin{aligned} &D_1^2 z + \left(1 - \frac{1}{2}(a\Omega)^2 - h\cos\omega T_1\right)z \\ &\quad - \big(\alpha - \beta z^2\big)D_1 z - \left(\gamma - \frac{1}{3}(a\Omega)^2\right)z^3 = 0. \end{aligned} \tag{10}$$

In (10), the influence of the frequency Ω is introduced in the natural frequency of the system and in the nonlinear stiffness coefficient as well. This equation can be written as

$$\ddot{z} + \big(\omega_0^2 - h\cos\omega t\big)z - \big(\alpha - \beta z^2\big)\dot{z} - \xi z^3 = 0 \tag{11}$$

where $\omega_0^2 = 1 - \frac{1}{2}(a\Omega)^2$, $\xi = \gamma - \frac{1}{3}(a\Omega)^2$ and an overdot denotes differentiation with respect to time t.

3 The 2:1 resonance

We express the 2:1 resonant condition by introducing a detuning parameter σ according to

$$\omega_0^2 = \frac{\omega^2}{4} + \sigma. \tag{12}$$

Following [26, 27], we apply a double perturbation technique by introducing two bookkeeping parameters μ and η. To implement the first perturbation to derive a slow flow, we use the parameter μ, and to investigate periodic solutions of the slow flow we use a second perturbation technique by considering the other parameter η.

3.1 Slow flow and entrainment

We rewrite (11) as

$$\ddot{z} + \frac{\omega^2}{4}z = \mu\big\{-\sigma z + \big(\alpha - \beta z^2\big)\dot{z} + \xi z^3 + hz\cos\omega t\big\}. \tag{13}$$

Using the multiple scales technique [28], we seek a solution to (13) in the form

$$z(t) = z_0(T_1, T_2) + \mu z_1(T_1, T_2) + O\big(\mu^2\big), \tag{14}$$

where $T_1 = t$ and $T_2 = \mu t$. In terms of the variables T_i, the time derivatives become $\frac{d}{dt} = D_1 + \mu D_2 + O(\mu^2)$ and $\frac{d^2}{dt^2} = D_1^2 + 2\mu D_1 D_2 + O(\mu^2)$ where $D_i^j = \frac{\partial^j}{\partial^j T_i}$. Substituting (14) into (13) and equating coefficients of like powers of μ, we obtain

– Order μ^0:

$$D_1^2 z_0 + \frac{\omega^2}{4}z_0 = 0. \tag{15}$$

– Order μ^1:

$$\begin{aligned} D_1^2 z_1 + \frac{\omega^2}{4}z_1 = &-2D_1 D_2 z_0 - \sigma z_0 \\ &+ \big(\alpha - \beta z_0^2\big)D_1 z_0 \\ &+ \xi z_0^3 + hz_0\cos\omega T_1. \end{aligned} \tag{16}$$

The solution to the first order is given by

$$z_0(T_1, T_2) = r(T_2)\cos\left(\frac{\omega}{2}T_1 + \theta(T_2)\right). \tag{17}$$

Substituting (17) into (16), removing secular terms and using the expressions $\frac{dr}{dt} = \mu D_2 r + O(\mu^2)$, $\frac{d\theta}{dt} = \mu D_2\theta + O(\mu^2)$, we obtain the slow flow modulation equations of amplitude and phase

$$\begin{aligned} \frac{dr}{dt} &= \frac{\alpha}{2}r - \frac{\beta}{8}r^3 - \frac{h}{2\omega}r\sin(2\theta), \\ \frac{d\theta}{dt} &= \frac{\sigma}{\omega} - \frac{3\xi}{4\omega}r^2 - \frac{h}{2\omega}\cos(2\theta). \end{aligned} \tag{18}$$

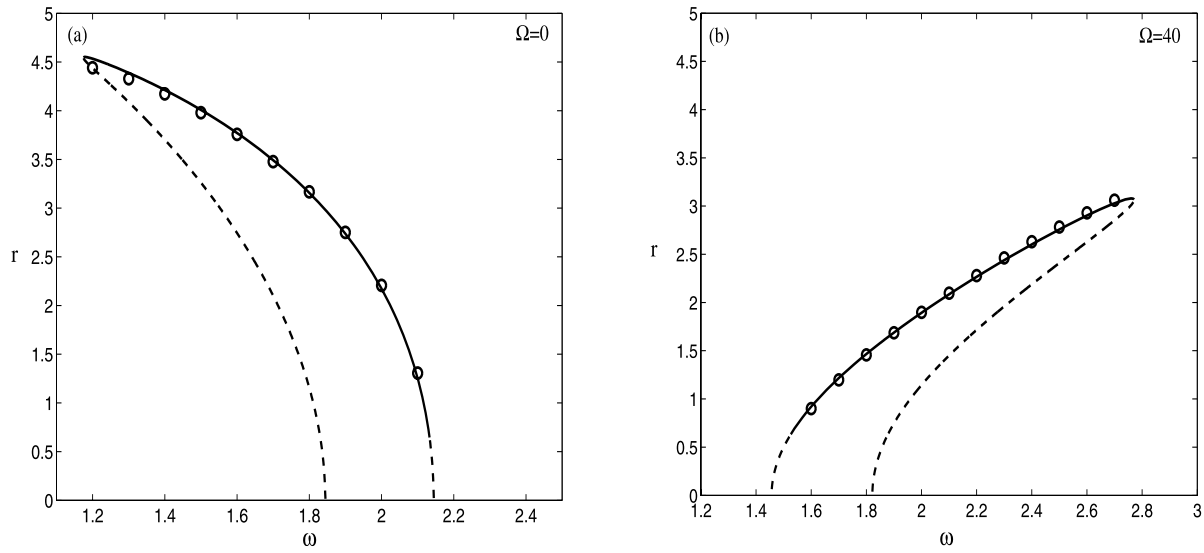

Fig. 1 Amplitude frequency response near 2:1 resonance. Analytical approximation: *Solid* (for stable) and *dashed* for (unstable). Numerical simulation: *circles*

This slow flow is invariant under the transformation $\theta \to -\theta + \frac{\pi}{2}$, $\sigma \to -\sigma$ and $\xi \to -\xi$. Thus, system (18) can take the form

$$\begin{aligned} \frac{dr}{dt} &= \frac{\alpha}{2}r - \frac{\beta}{8}r^3 - \frac{h}{2\omega}r\sin(2\theta), \\ \frac{d\theta}{dt} &= \frac{s\sigma}{\omega} - \frac{3s\xi}{4\omega}r^2 - \frac{h}{2\omega}\cos(2\theta), \end{aligned} \tag{19}$$

where $s = \pm 1$. Equilibrium points of the slow flow (19), corresponding to periodic oscillations of (11), are determined by setting $\frac{dr}{dt} = \frac{d\theta}{dt} = 0$. Using the relation $\cos^2\theta + \sin^2\theta = 1$ and we define $\rho = r^2$, we obtain the following quadratic equation in ρ

$$\left(\frac{\beta^2}{64} + \frac{9\xi^2}{16\omega^2}\right)\rho^2 - \left(\frac{\alpha\beta}{8} + \frac{3\sigma\xi}{2\omega^2}\right)\rho + \frac{\alpha^2}{4} + \frac{\sigma^2}{\omega^2} - \frac{h^2}{4\omega^2} = 0. \tag{20}$$

Equation (20) has two real roots if the discriminant Δ is nonnegative. This gives the condition

$$\Delta = \left(\frac{\alpha\beta}{16} + \frac{3\sigma\xi}{4\omega^2}\right)^2 - \left(\frac{\beta^2}{64} + \frac{9\xi^2}{16\omega^2}\right)\left(\frac{\alpha^2}{4} + \frac{\sigma^2}{\omega^2} - \frac{h^2}{4\omega^2}\right) > 0. \tag{21}$$

These solutions are positive if the two following conditions are held

$$\begin{aligned} C &= \frac{\alpha^2}{4} + \frac{\sigma^2}{\omega^2} - \frac{h^2}{4\omega^2} > 0, \\ B &= \frac{\alpha\beta}{4} + \frac{3\sigma\xi}{\omega^2} > 0. \end{aligned} \tag{22}$$

Furthermore, (20) has only one positive root if

$$C = \frac{\alpha^2}{4} + \frac{\sigma^2}{\omega^2} - \frac{h^2}{4\omega^2} < 0. \tag{23}$$

In what follows, we fix the parameters $\alpha = 0.01$, $\beta = 0.05$, $\gamma = 0.04$, $h = 0.3$ and $a = 0.02$.

In Fig. 1a the frequency response curve, as given by (20), is presented for $\Omega = 0$. The effect of the excitation frequency Ω on the frequency-locking area is illustrated in Fig. 1b for $\Omega = 40$. It can be seen that as the frequency Ω increases, the entrainment area shifts left and the nonlinear characteristic stiffness changes causing the system to switch from softening to hardening behavior. Analytical approximations (solid line for stable oscillations and dashed line for unstable ones) are compared to numerical integration (circles) using a Runge–Kutta method.

Figure 2a illustrates the bifurcation curves of periodic solutions of the slow dynamic (11) for $\Omega = 0$. We can distinct four regions. In region I, where conditions

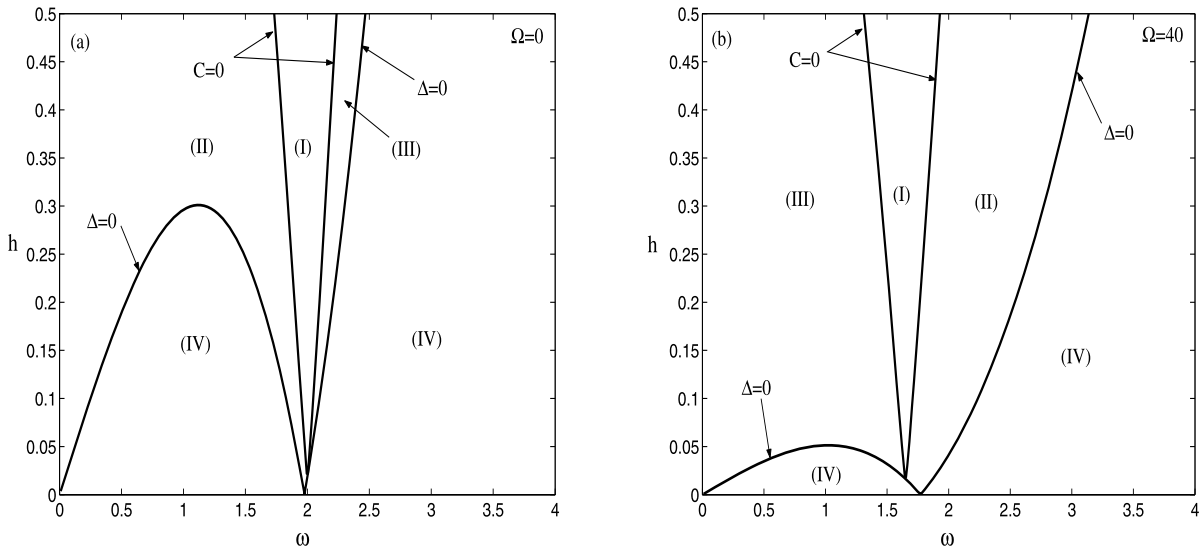

Fig. 2 Bifurcation curves of periodic solutions of the slow dynamic (11) near 2:1 resonance

(21) and (23) are satisfied, there are two possible solutions: an unstable trivial solution and a larger stable one. Within region II, where conditions (21) and (22) are satisfied, there are three possible solutions: one unstable, one larger stable and the trivial unstable solution. Within the regions III and IV only an unstable trivial solution exists. In these regions, a limit cycle exists and it is stable. Figure 2b is plotted for $\Omega = 40$ showing the effect of Ω on the bifurcation curves. It can be seen that as Ω increases, region I jumps from the right branch of the curve $\Delta = 0$ to the left one causing an exchange between regions II and III inside the curve $\Delta = 0$. This behavior is consistent with the change of the backbone curve in Fig. 1.

3.2 Slow slow flow and limit cycle

In this section, we construct analytical approximation of the limit cycle of the slow flow (19) corresponding to quasi-periodic motion of the slow dynamic (11). We transform the polar form (19) using the variable change

$$u = r\cos\theta, \quad v = -r\sin\theta \tag{24}$$

to the Cartesian system

$$\begin{aligned}
\frac{du}{dt} &= \left(\frac{s\sigma}{\omega} + \frac{h}{2\omega}\right)v \\
&\quad + \eta\left\{\frac{\alpha}{2}u - \left(\frac{\beta}{8}u + \frac{3s\xi}{4\omega}v\right)\left(u^2+v^2\right)\right\}, \\
\frac{dv}{dt} &= -\left(\frac{s\sigma}{\omega} - \frac{h}{2\omega}\right)u \\
&\quad + \eta\left\{\frac{\alpha}{2}v - \left(\frac{\beta}{8}v - \frac{3s\xi}{4\omega}u\right)\left(u^2+v^2\right)\right\},
\end{aligned} \tag{25}$$

where the parameter η is introduced in the damping and nonlinearity to implement the second perturbation method. Approximation of periodic solutions of the slow flow (25) can be obtained by using a multiple scales perturbation technique [26, 27]. We expand solutions as

$$\begin{aligned}
u(t) &= u_0(T_1,T_2) + \eta u_1(T_1,T_2) + O\left(\eta^2\right), \\
v(t) &= v_0(T_1,T_2) + \eta v_1(T_1,T_2) + O\left(\eta^2\right),
\end{aligned} \tag{26}$$

where $T_1 = t$ and $T_2 = \eta t$. Introducing $D_i = \frac{\partial}{\partial T_i}$ yields $\frac{d}{dt} = D_1 + \eta D_2 + O(\eta^2)$, substituting (26) into (25) and collecting terms, we get

– Order η^0:

$$\begin{aligned}
&D_1^2 u_0 + v^2 u_0 = 0, \\
&\left(\tfrac{s\sigma}{\omega} + \tfrac{h}{2\omega}\right)v_0 = D_1 u_0.
\end{aligned} \tag{27}$$

– Order η^1:

$$D_1^2 u_1 + v^2 u_1$$

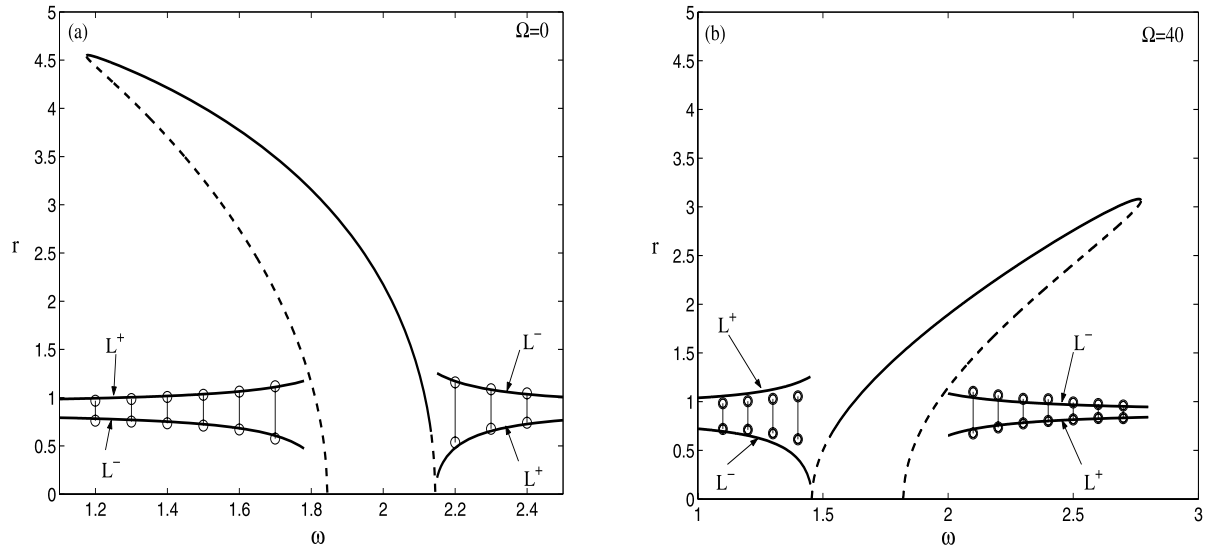

Fig. 3 Effect of the frequency Ω on the entrainment area and on the modulation amplitude vibration for the 2:1 resonance

$$
\begin{aligned}
&= \left(\frac{s\sigma}{\omega}+\frac{h}{2\omega}\right)\left[-D_2v_0+\frac{\alpha}{2}v_0\right.\\
&\quad\left.-\left(\frac{\beta}{8}v_0-\frac{3s\xi}{4\omega}u_0\right)\left(u_0^2+v_0^2\right)\right]\\
&\quad-D_1D_2u_0+\frac{\alpha}{2}D_1u_0\\
&\quad-D_1\left[\left(\frac{\beta}{8}u_0+\frac{3s\xi}{4\omega}v_0\right)\left(u_0^2+v_0^2\right)\right],\\
&\left(\frac{s\sigma}{\omega}+\frac{h}{2\omega}\right)v_1\\
&\quad=D_1u_1+D_2u_0-\frac{\alpha}{2}u_0\\
&\quad+\left(\frac{\beta}{8}u_0+\frac{3s\xi}{4\omega}v_0\right)\left(u_0^2+v_0^2\right),
\end{aligned}
\tag{28}
$$

where $\nu=\sqrt{(\frac{\sigma}{\omega})^2-(\frac{h}{2\omega})^2}$ is the proper frequency of system (25) corresponding to the frequency of slow flow limit cycle. The solution to the first order system (27) is given by

$$
\begin{aligned}
u_0(T_1,T_2)&=R(T_2)\cos\big(\nu T_1+\varphi(T_2)\big),\\
v_0(T_1,T_2)&=-\frac{\nu}{(\frac{s\sigma}{\omega}+\frac{h}{2\omega})}R(T_2)\sin\big(\nu T_1+\varphi(T_2)\big).
\end{aligned}
\tag{29}
$$

Substituting (29) into (28) and removing secular terms gives the following autonomous slow slow (s.s.) flow system on R and φ

$$
\begin{aligned}
\frac{dR}{dt}&=\frac{\alpha}{2}R-\frac{s\beta\sigma}{8s\sigma+4h}R^3,\\
\frac{d\varphi}{dt}&=-\frac{3s\xi(8\sigma^2+h^2)}{8\omega(2s\sigma+h)\sqrt{4\sigma^2-h^2}}R^2.
\end{aligned}
\tag{30}
$$

Equilibria in (30) are obtained by setting $\frac{dR}{dt}=0$ and given by

$$
R=0,\quad R=\sqrt{\frac{2\alpha(2s\sigma+h)}{s\beta\sigma}}.
\tag{31}
$$

The nontrivial equilibrium in (31) will correspond to the amplitude of the limit cycle of the slow flow (25) and to quasi-periodic oscillations in the slow dynamic (11). In Figs. 3a, b we draw for the two different values $\Omega=0$ and $\Omega=40$ the analytical amplitude of the slow flow limit cycle, (31), and the entrainment area as given by (20). The curves labelled L^+ correspond to $s=+1$ in (31) and the curves labeled L^- correspond to $s=-1$. The numerical modulation amplitude vibrations (quasi-periodic oscillations) are marked with double circles connected with a vertical line. Comparison between analytical results and numerical integration of the modulation amplitude motion shows a good agreement.

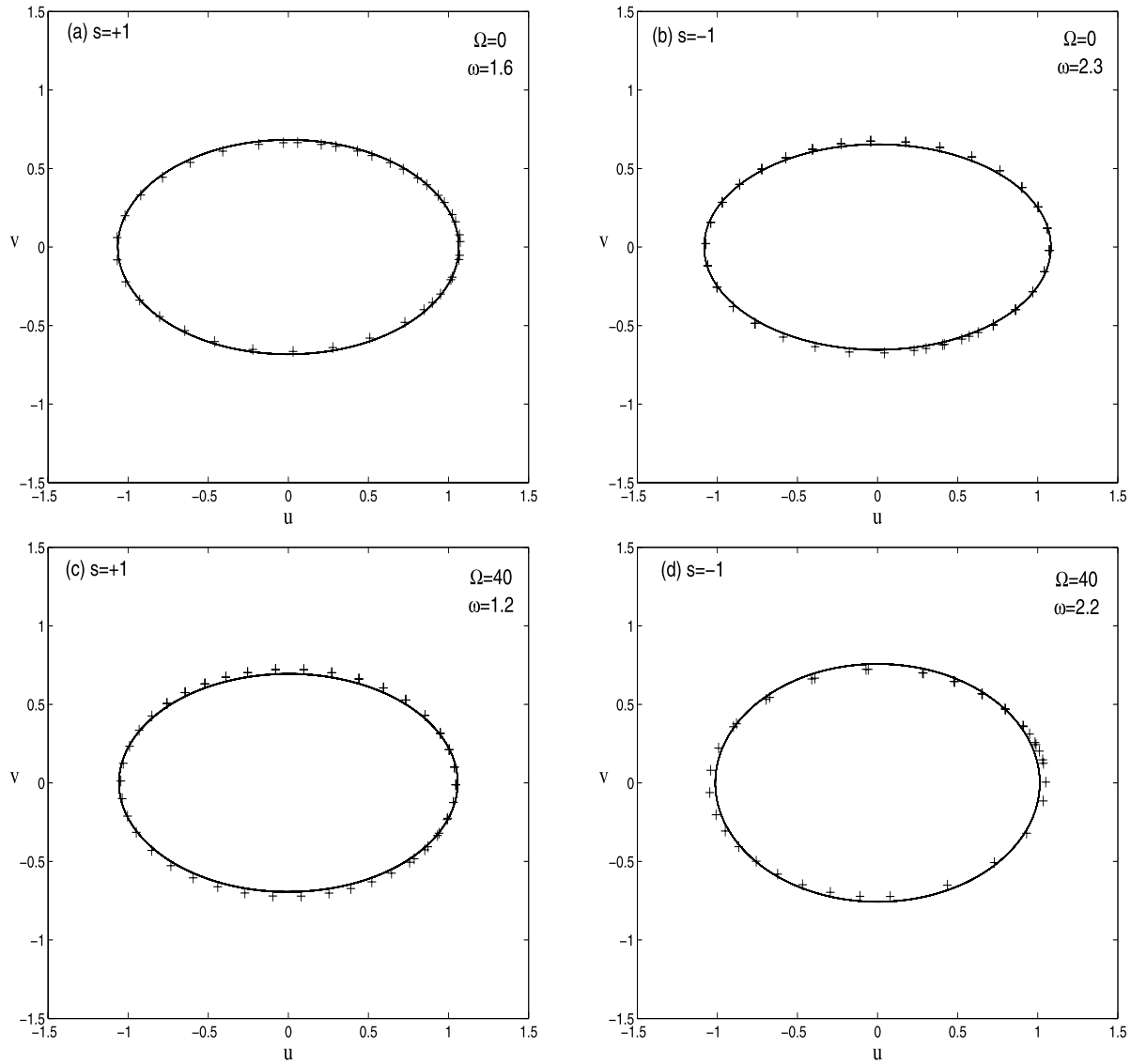

Fig. 4 Comparison between analytical approximation (*solid line*) of periodic solution, (32), and numerical integration (*plus signs*) of the slow flow (25) near the 2:1 resonance

The approximate periodic solution of the slow flow system (25) is written as

$$u(t) = R\cos(\nu t + \varphi),$$
$$v(t) = -\frac{2\nu\omega}{(2s\sigma + h)} R\sin(\nu t + \varphi), \tag{32}$$

where φ is given by (30). To validate the analytical finding, we show in Fig. 4 comparison between the approximate periodic solution (32) and the numerical integration of the slow flow (25) using a Runge–Kutta method. Figures 4a, c are plotted for $s = +1$ and Figs. 4b, d are plotted for $s = -1$.

The approximate quasi-periodic oscillation of the slow dynamic system (11) is written as

$$z(t) = u(t)\cos\left(\frac{\omega}{2}t\right) + v(t)\sin\left(\frac{\omega}{2}t\right). \tag{33}$$

Finally, the *quasi* quasi-periodic response of the original system (1) is given by (2), (7) and (33). In Fig. 5, we present examples of time histories of the slow dy-

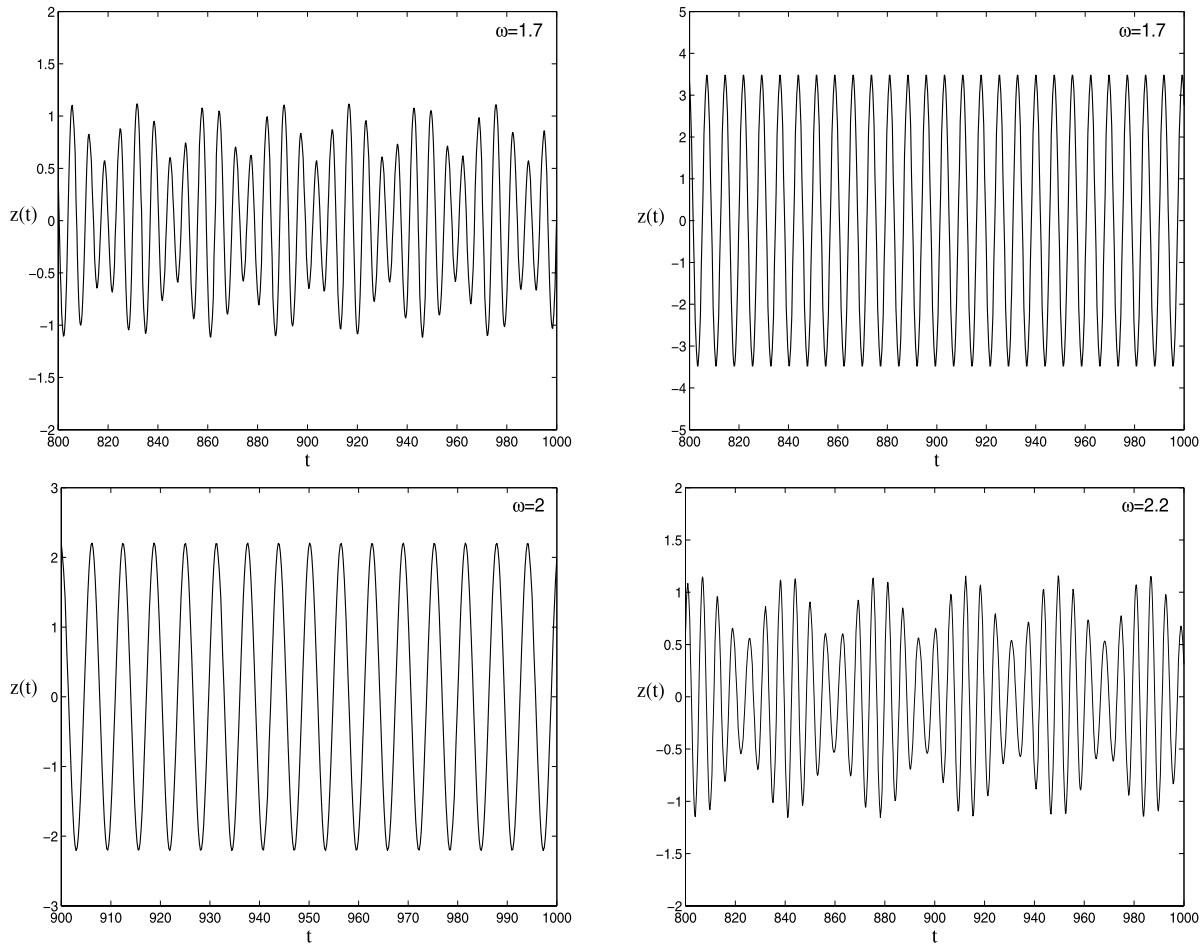

Fig. 5 Examples of time histories of the slow dynamic $z(t)$ by numerical integration of system (11) for $\Omega = 0$

namic $z(t)$ obtained by numerical simulation of system (25) for some values of ω picked from Fig. 3a.

4 The 1:1 resonance

We express the 1:1 resonant condition by introducing a detuning parameter σ according to

$$\omega_0^2 = \omega^2 + \sigma \tag{34}$$

and we introduce a bookkeeping parameter μ such that (11) is rewritten as

$$\ddot{z} + \omega^2 z = \mu\left\{-\sigma z + \alpha\dot{z} - \beta z^2\dot{z} + \xi z^3 + hz\cos\omega t\right\}. \tag{35}$$

4.1 Slow flow and entrainment

Using the multiple scales technique, we seek a solution to (35) in the form

$$z(t) = z_0(T_1, T_2, T_3) + \mu z_1(T_1, T_2, T_3) + \mu^2 z_2(T_1, T_2, T_3) + O\left(\mu^3\right), \tag{36}$$

where $T_1 = t$, $T_2 = \mu t$ and $T_3 = \mu^2 t$. In terms of the variables T_i, the time derivatives become $\frac{d}{dt} = D_1 + \mu D_2 + \mu^2 D_3 + O(\mu^3)$ and $\frac{d^2}{dt^2} = D_1^2 + 2\mu D_1 D_2 + \mu^2(2D_1 D_3 + D_2^2) + O(\mu^3)$ where $D_i^j = \frac{\partial^j}{\partial^j T_i}$. Substituting (36) into (35) and equating coefficients of like powers of μ, we obtain

– Order μ^0:

$$D_1^2 z_0 + \omega^2 z_0 = 0. \tag{37}$$

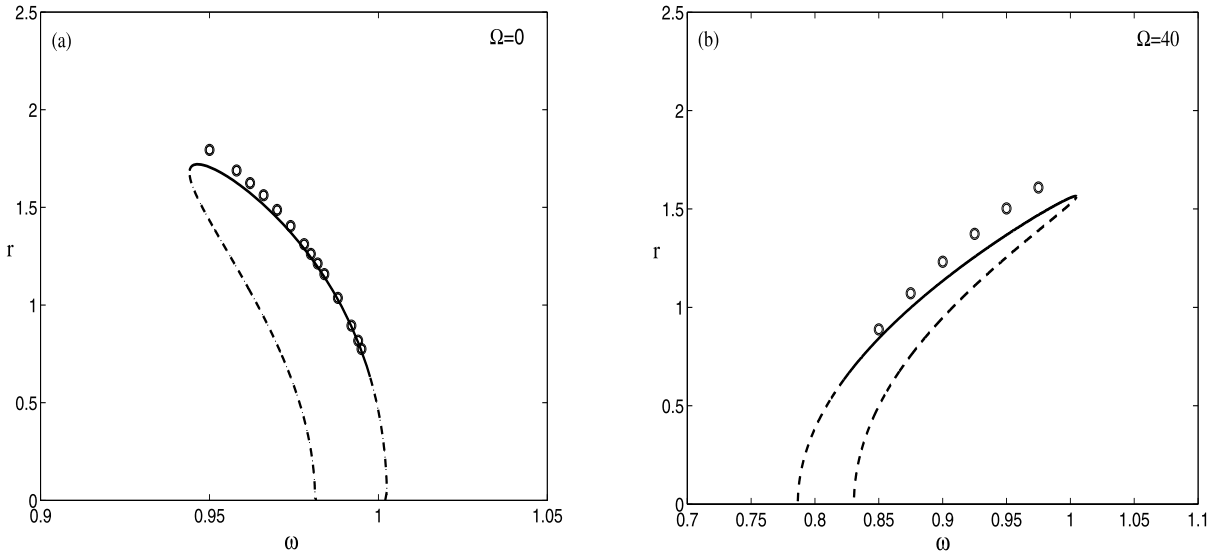

Fig. 6 Amplitude frequency response near 1:1 resonance. Analytical approximation: *Solid* (for stable) and *dashed* for (instable). Numerical simulation: *circles*

– Order μ^1:

$$D_1^2 z_1 + \omega^2 z_1 = -\sigma z_0 + \alpha D_1 z_0 - \beta z_0^2 D_1 z_0 + \xi z_0^3 + h z_0 \cos\omega T_1 - 2D_1 D_2 z_0. \tag{38}$$

– Order μ^2:

$$\begin{aligned} &D_1^2 z_2 + \omega^2 z_2 \\ &\quad = \big(-\sigma - 2\beta z_0 D_1 z_0 + 3\xi z_0^2 + h\cos\omega T_1\big) z_1 \\ &\qquad + \big(\alpha - \beta z_0^2\big)(D_1 z_1 + D_2 z_0) \\ &\qquad - 2D_1 D_3 z_0 - 2D_1 D_2 z_1 - D_2^2 z_0. \end{aligned} \tag{39}$$

The solution to the first order is given by

$$z_0(T_1, T_2, T_3) = r(T_2, T_3)\cos\big(\omega T_1 + \theta(T_2, T_3)\big). \tag{40}$$

Substituting (40) into (38) and (39) and removing secular terms, we obtain the modulation equations

$$\begin{aligned} D_2 r &= \frac{\alpha}{2} r - \frac{\beta}{8} r^3, \\ D_3 r &= \frac{3\alpha\xi}{16\omega^2} r^3 - \frac{h^2}{8\omega^3} r \sin(2\theta), \\ D_2\theta &= \frac{\sigma}{2\omega} - \frac{3\xi}{8\omega} r^2, \end{aligned} \tag{41}$$

$$\begin{aligned} D_3\theta = &-\frac{\sigma^2}{8\omega^3} - \frac{\alpha^2}{8\omega} - \frac{h^2}{12\omega^3} \\ &+ \left(\frac{\alpha\beta}{8\omega} + \frac{3\sigma\xi}{16\omega^3}\right) r^2 - \frac{h^2}{8\omega^3}\cos(2\theta). \end{aligned} \tag{42}$$

Combining (41) and (42) into the expressions $\frac{dr}{dt} = \mu D_2 r + \mu^2 D_3 r$, $\frac{d\theta}{dt} = \mu D_2\theta + \mu^2 D_3\theta$, we obtain the following slow flow modulation equations of amplitude and phase

$$\begin{aligned} \frac{dr}{dt} &= A_0 r - A_1 r^3 - H r \sin(2\theta), \\ \frac{d\theta}{dt} &= B_0 - B_1 r^2 - H\cos(2\theta), \end{aligned} \tag{43}$$

where $A_0 = \frac{\alpha}{2}$, $A_1 = \frac{\beta}{8} - \frac{3\alpha\xi}{16\omega^2}$, $B_0 = \frac{\sigma}{2\omega} - \frac{\sigma^2}{8\omega^3} - \frac{\alpha^2}{8\omega} - \frac{h^2}{12\omega^3}$, $B_1 = \frac{3\xi}{8\omega} - \frac{\alpha\beta}{8\omega} - \frac{3\sigma\xi}{16\omega^3}$ and $H = \frac{h^2}{8\omega^3}$. Periodic oscillations of (11) are given by setting in (43) $\frac{dr}{dt} = \frac{d\theta}{dt} = 0$. Using the relation $\cos^2\theta + \sin^2\theta = 1$ and we define $\rho = r^2$, we obtain the following quadratic equation in ρ

$$\begin{aligned} &\big(A_1^2 + B_1^2\big)\rho^2 - 2(A_0 A_1 + B_0 B_1)\rho \\ &\quad + A_0^2 + B_0^2 - H^2 = 0, \end{aligned} \tag{44}$$

which has two real roots if the discriminant Δ is non-negative. This gives the condition

$$\Delta = (A_0 A_1 + B_0 B_1)^2$$

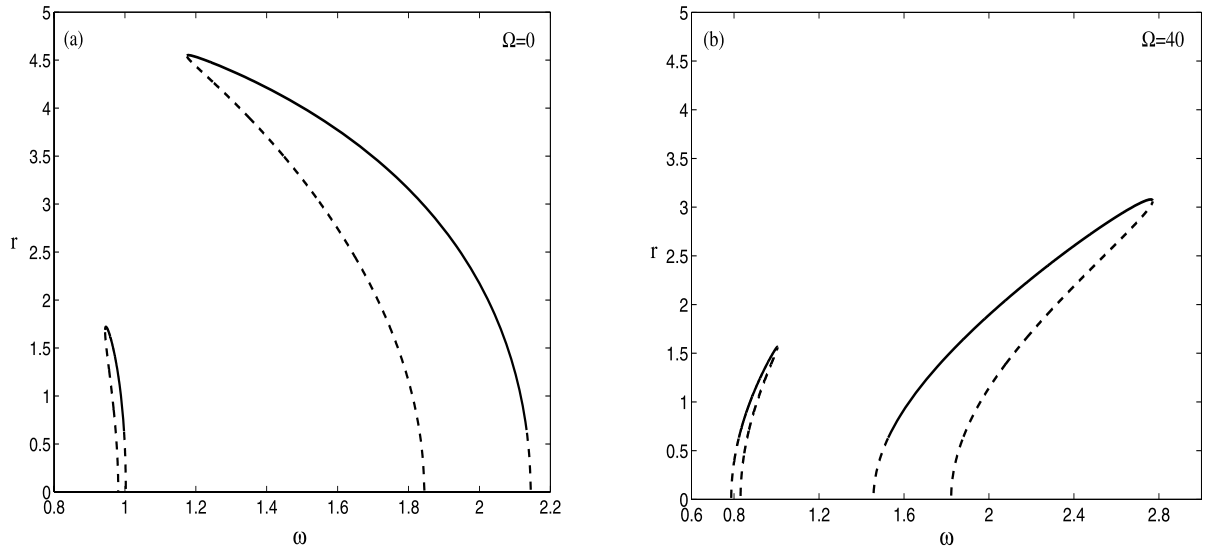

Fig. 7 Amplitude frequency response near 1:1 and 2:1 resonances. Analytical approximation: *Solid* (for stable) and *dashed* for (unstable)

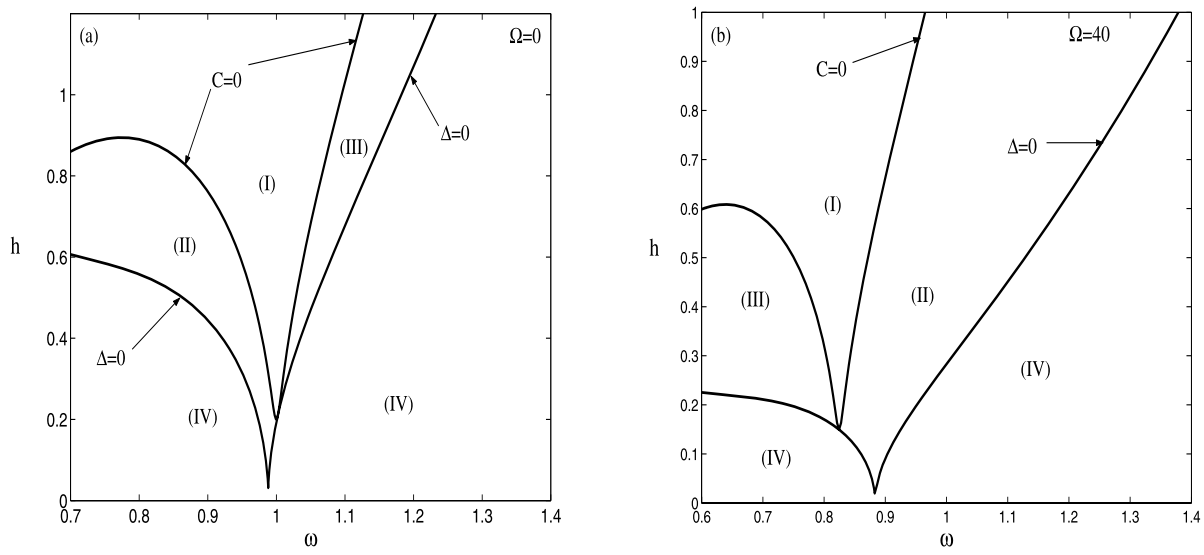

Fig. 8 Bifurcation curves of periodic solutions of the slow dynamic (11) near 1:1 resonance

$$-\left(A_1^2+B_1^2\right)\left(A_0^2+B_0^2-H^2\right)>0. \tag{45}$$

These two solutions are positive if the two following conditions are held

$$\begin{aligned} C&=A_0^2+B_0^2-H^2>0,\\ B&=A_0A_1+B_0B_1>0. \end{aligned} \tag{46}$$

Equation (44) has only one positive root if

$$C=A_0^2+B_0^2-H^2<0. \tag{47}$$

In Fig. 6, we present the frequency response curves near the resonance 1:1, as given by (44), for $\Omega=0$ and $\Omega=40$. As for the 2:1 resonance case, increasing the frequency Ω shifts the entrainment area left and changes the nonlinear characteristic stiffness. Com-

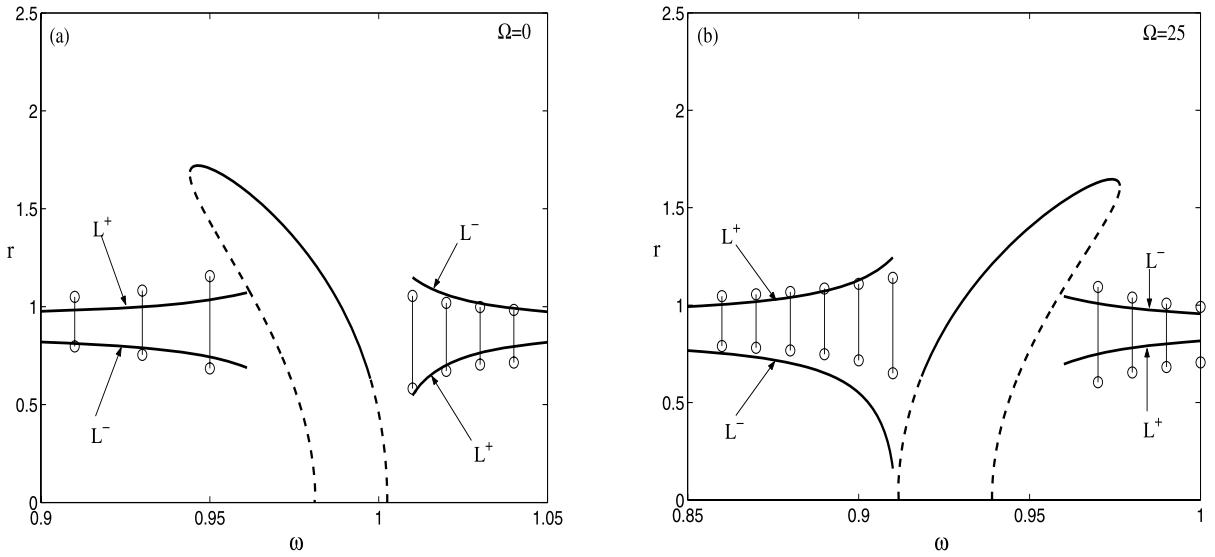

Fig. 9 Effect of the frequency Ω on the entrainment area and on the modulation amplitude vibration near 1:1 resonance

parisons between analytical approximations (solid and dashed line) and numerical integration (circles) using a Runge–Kutta method is provided. Figure 7 illustrates the frequency response curves for both 1:1 and 2:1 resonances offering a global view of the two entrainment regions.

Figure 8 illustrates the bifurcation curves of periodic solutions of the slow dynamic (11) for $\Omega = 0$ and $\Omega = 40$. Note that the dynamic here is similar to that of the 2:1 resonance case. Figure 8b plotted for $\Omega = 40$ shows the effect of Ω on the bifurcation curves. Similar behavior as for the 2:1 resonance can be seen, that is, as Ω increases, region I switches from the right branch of the curve $\Delta = 0$ to the left one causing an exchange between regions II and III inside the curve $\Delta = 0$.

4.2 Slow slow flow and limit cycle

Following the same analysis as for the 2:1 resonance case, we construct analytical approximation of the limit cycle of the slow flow (43) corresponding to quasi-periodic motion of the slow dynamic (11) near the 1:1 resonance.

The Cartesian system corresponding to the polar form (43) is written as

$$\begin{aligned}\frac{du}{dt} &= (B_0 + H)v \\ &\quad + \eta\{A_0 u - (A_1 u + B_1 v)(u^2 + v^2)\}, \\ \frac{dv}{dt} &= -(B_0 - H)u \\ &\quad + \eta\{A_0 v - (A_1 v - B_1 u)(u^2 + v^2)\},\end{aligned} \tag{48}$$

where the parameter η is introduced in the damping and nonlinearity to implement the second perturbation step. Using the multiple scales method, the solution to the first order of system (48) is given by

$$\begin{aligned}u_0(t) &= R\cos(\nu t + \varphi), \\ v_0(t) &= -\frac{\nu}{(B_0 + H)} R\sin(\nu t + \varphi),\end{aligned} \tag{49}$$

where $\nu = \sqrt{B_0^2 - H^2}$ is the proper frequency of system (48) corresponding to the frequency of slow flow limit cycle. The amplitude R and the phase φ vary with time according to the following autonomous s.s. flow system

$$\begin{aligned}\frac{dR}{dt} &= A_0 R - \frac{B_0 A_1}{B_0 + H} R^3, \\ \frac{d\varphi}{dt} &= -\frac{B_1(2B_0^2 + H^2)}{2(B_0 + H)\sqrt{B_0^2 - H^2}} R^2.\end{aligned} \tag{50}$$

Equilibria in (50) are given by

$$R = 0, \qquad R = \sqrt{\frac{A_0(B_0 + H)}{B_0 A_1}}. \tag{51}$$

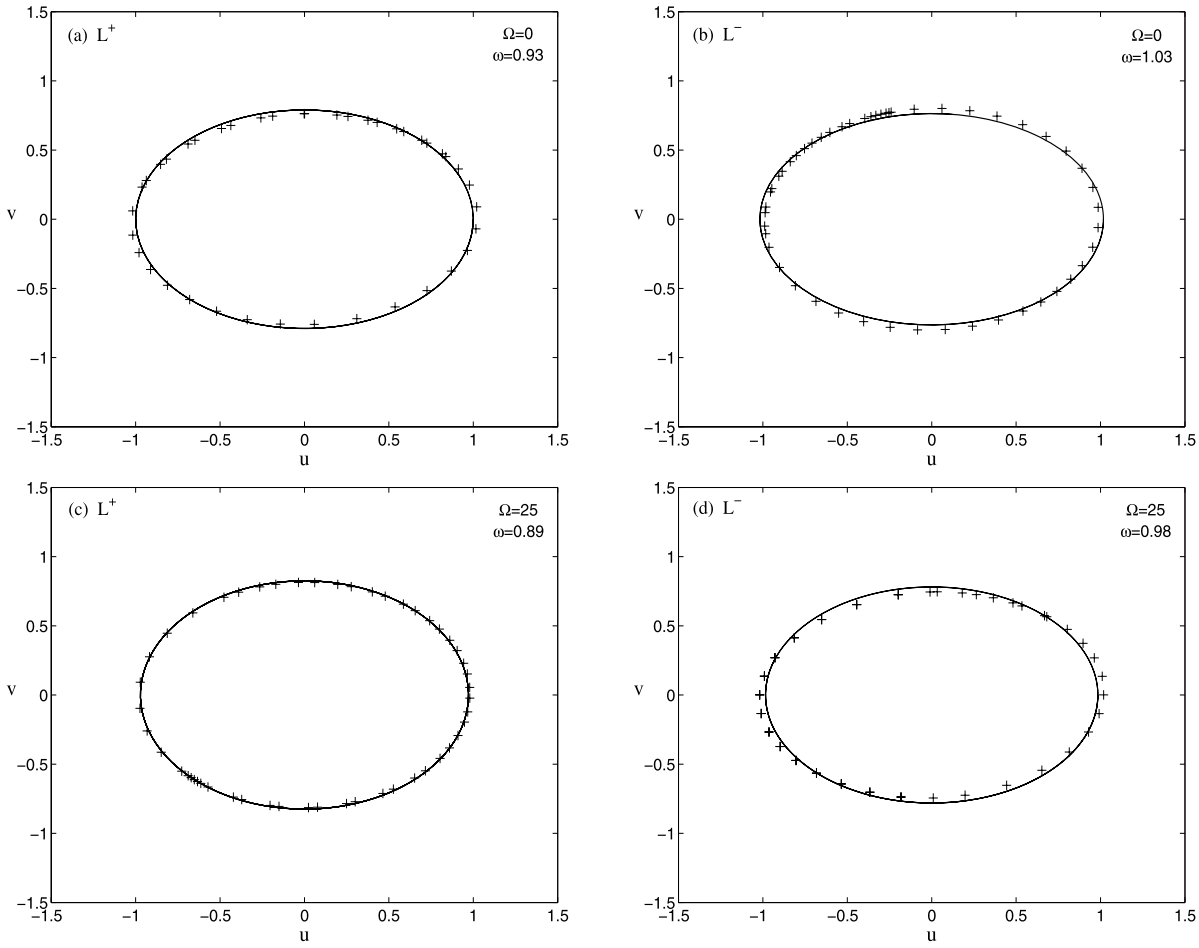

Fig. 10 Comparison between analytical approximation (*solid line*) of periodic solution, (49), and numerical integration (*plus signs*) of the slow flow (48)

The nontrivial equilibrium in (51) corresponds to the amplitude of the limit cycle of the slow flow (43) and to quasi-periodic oscillations in the slow dynamic (11).

In Figs. 9a, b we draw for the two different values $\Omega = 0$ and $\Omega = 25$ the analytical amplitude of the slow flow limit cycle, (51), and the entrainment area as given by (44).

The analytical expression of the limit cycle amplitude, (51), provides the curves labeled L^+. However, the curves labeled L^- can be obtained following a similar reasoning as for the 2:1 resonance case. In fact, since system (43) has the same form as system (18), the invariance of system (18) under transformation $\sigma \to -\sigma$, $\xi \to -\xi$ and $\theta \to \frac{\pi}{2} - \theta$ can be obtained in system (43) with the transformation $B_0 \to -B_0$, $B_1 \to -B_1$ and $\theta \to \frac{\pi}{2} - \theta$. In this case, the analytical limit cycle amplitude, (51), can take the form

$$R = \sqrt{\frac{A_0(sB_0 + H)}{sB_0A_1}}. \tag{52}$$

Hence, the curves L^- can be obtained by setting $s = -1$ in (52); see Fig. 9.

The numerical modulation amplitude vibrations (double circles connected with a vertical line) and the analytical results (solid lines) are shown for comparison. Figure 10 shows comparison between the approximate periodic solution, (49), and the numerical integration of the slow flow (48) using a Runge–Kutta method. Figures 10a, c are plotted for L^+ and Figs. 10b, d are plotted for L^-. Finally, Fig. 11 gives

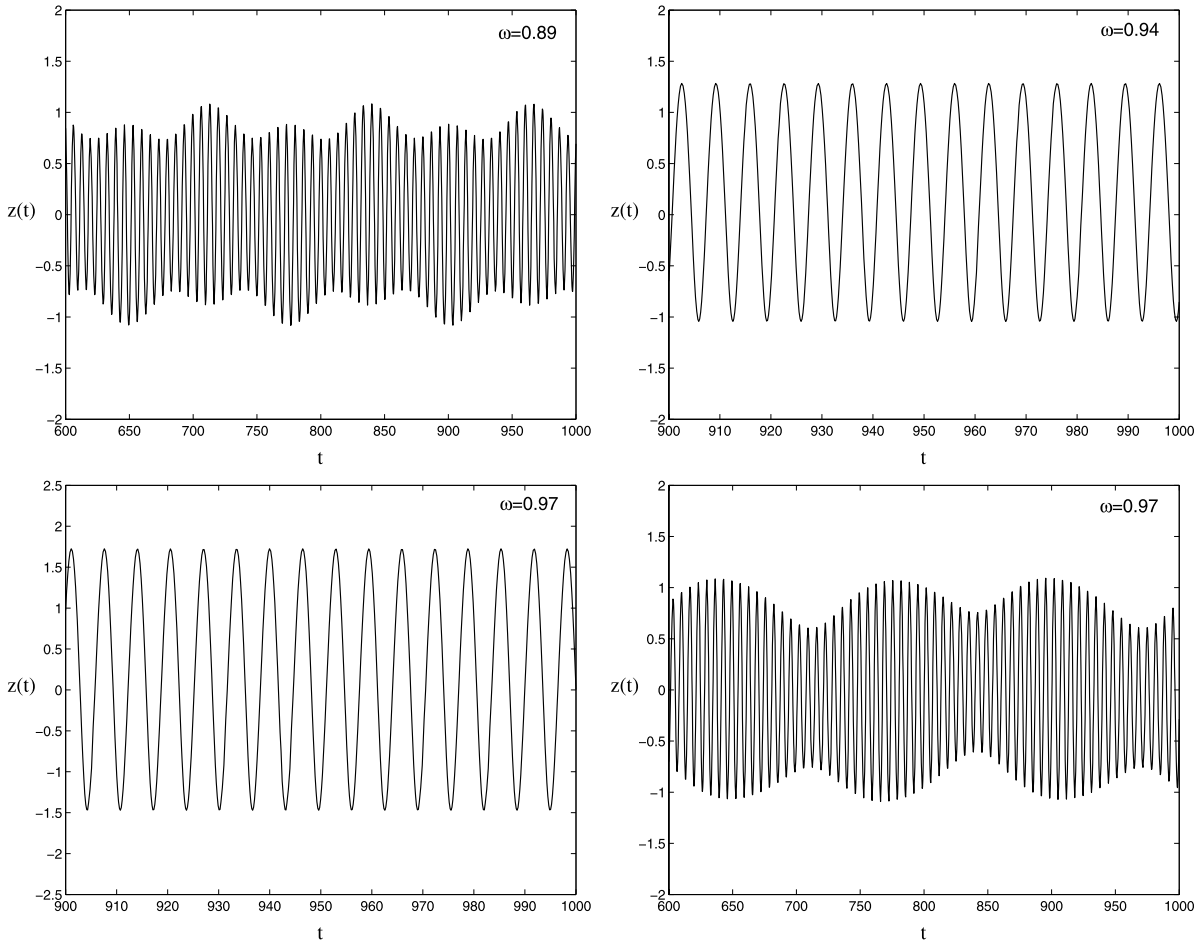

Fig. 11 Examples of time histories of the slow dynamic $z(t)$, near 1:1 resonance, by numerical integration of (11) for $\Omega = 25$

examples of time histories of the slow dynamic $z(t)$ near 1:1 resonance obtained by numerical simulation of (11) for some values of ω picked from Fig. 9b.

5 Conclusion

The influence of a FHE on the frequency-locking area of 2:1 and 1:1 resonances in a van der Pol–Mathieu–Duffing oscillator has been studied analytically and numerically. The application of the DPM technique followed by two successive multiple scales methods reduces successively the original oscillator to a slow dynamic, a slow flow and an s.s. flow. The analysis of equilibria of slow flow and s.s. flow provides information on periodic and quasi-periodic oscillations of the slow motion of the system, respectively. Results show that in both resonance cases FHE can change the nonlinear characteristic spring behavior of the system and causes the entrainment area to shift. In contrast, no significant effect on the amplitudes of both entrained and quasi-periodic responses is noticed. This result suggests that controlling and adjusting the entrainment area to a desired frequency range for a considered resonance may be achieved by acting only on the fast frequency excitation Ω. This study shows also that entrained vibrations with moderate amplitudes can be achieved in a narrow zone near the 1:1 resonance. In contrast, the entrained motions near the 2:1 resonance can have relatively large amplitudes (Fig. 7). This result of realizing entrained vibrations with relatively small amplitude may be of interest from engineering applications point of view.

References

1. Tondl, A.: On the interaction between self-excited and parametric vibrations. National Research Institute for Machine Design, Monographs and Memoranda No. 25, Prague (1978)
2. Schmidt, G.: Interaction of self-excited forced and parametrically excited vibrations. In: The 9th International Conference on Nonlinear Oscillations. Application of The Theory of Nonlinear Oscillations, vol. 3. Naukowa Dumka, Kiev (1984)
3. Szabelski, K., Warminski, J.: Self excited system vibrations with parametric and external excitations. J. Sound. Vib. **187**(4), 595–607 (1995)
4. Szabelski, K., Warminski, J.: The nonlinear vibrations of parametrically self-excited system with two degrees of freedom under external excitation. Nonlinear Dyn. **14**, 23–36 (1997)
5. Belhaq, M., Clerc, R.L., Hartman, C.: Etude numérique d'une 4-résonance d'une équation de Liénard forcée. C.R. Acad. Sci. Paris **303**(II-10), 873–876 (1986)
6. Belhaq, M.: Numerical study for parametric excitation of differential equation near a 4-resonance. Mech. Res. Commun. **17**(4), 199–206 (1990)
7. Belhaq, M., Fahsi, A.: Higher-order approximation of subharmonics close to strong resonances in the forced oscillators. Comput. Math. Appl. **33**(8), 133–144 (1997)
8. Yano, S.: Analytic research on dynamic phenomena of parametrically and self-exited mechanical systems. Ing. Arch. **57**, 51–60 (1987)
9. Yano, S.: Considerations on self- and parametrically excited vibrational systems. Ing. Arch. **59**, 285–295 (1989)
10. Abouhazim, N., Belhaq, M., Lakrad, F.: Three-period quasi-periodic solutions in self-excited quasi-periodic Mathieu oscillator. Nonlinear Dyn. **39**, 395–409 (2005)
11. Pandey, M., Rand, R.H., Zehnder, A.: Perturbation analysis of entrainment in a micromechanical limit cycle oscillator. Commun. Nonlinear. Sci. Numer. Simul. **12**, 1291–1301 (2007)
12. Pandey, M., Rand, R.H., Zehnder, A.: Frequency locking in a forced Mathieu–van der Pol–Duffing system. Nonlinear Dyn. (2007), doi:10.1007/s11071-007-9238-x
13. Chelomei, V.N.: Mechanical paradoxes caused by vibrations. Sov. Phys. Dokl. **28**, 387–390 (1983)
14. Tcherniak, D.: The influence of fast excitation on a continuous system. J. Sound. Vib. **227**(2), 343–360 (1999)
15. Thomsen, J.J.: Some general effects of strong high-frequency excitation: stiffening, biasing, and smoothening. J. Sound. Vib. **253**(4), 807–831 (2002)
16. Jensen, J.S., Tcherniak, D.M., Thomsen, J.J.: Stiffening effects of high-frequency excitation: experiments for an axially loaded beam. J. Appl. Mech. **67**(2), 397–402 (2000)
17. Hansen, M.H.: Effect of high-frequency excitation on natural frequencies of spinning discs. J. Sound. Vib. **234**(4), 577–589 (2000)
18. Chatterjee, S., Singha, T.K., Karmakar, S.K.: Non-trivial effect of fast vibration on the dynamics of a class of nonlinearly damped mechanical systems. J. Sound. Vib. **260**(4), 711–730 (2003)
19. Thomsen, J.J.: Using fast vibrations to quench friction-induced oscillations. J. Sound. Vib. **228**(5), 1079–1102 (1999)
20. Thomsen, J.J., Fidlin, A.: Analytical approximations for stick-slip vibration amplitudes. Nonlinear Mech. **38**, 389–403 (2003)
21. Mann, B.P., Koplow, M.A.: Symmetry breaking bifurcations of a parametrically excited pendulum. Nonlinear Dyn. **46**, 427–437 (2006)
22. Sah, S.M., Belhaq, M.: Effect of vertical high-frequency parametric excitation on self-excited motion in a delayed van der Pol oscillator. Chaos, Solitons Fractals (2006), doi:10.1016/j.chaos.2006.10.040
23. Belhaq, M., Sah, S.M.: Horizontal fast excitation in delayed van der Pol oscillator. Commun Nonlinear. Sci. Numer. Simul. (2007), doi:10.1016/j.cnsns.2007.02.007
24. Thomsen, J.J.: Slow high-frequency effects in mechanics: problems, solutions, potentials. Int. J. Bif. Chaos **15**(9), 2799–2818 (2005)
25. Blekhman, I.I.: Vibrational Mechanics—Nonlinear Dynamic Effects, General Approach, Application. World Scientific, Singapore (2000)
26. Belhaq, M., Houssni, M.: Quasi-periodic oscillations, chaos and suppression of chaos in a nonlinear oscillator driven by parametric and external excitations. Nonlinear Dyn. **18**, 1–24 (1999)
27. Rand, R.H., Guennoun, K., Belhaq, M.: 2:2:1 Resonance in the quasi-periodic Mathieu equation. Nonlinear Dyn. **31**, 187–193 (2003)
28. Nayfeh, A.H., Mook, D.T.: Nonlinear Oscillations. Wiley, New York (1979)